Thermal stability and electrical properties of copper nitride with In or Ti*

Du Yun(杜 允)[a)b)], Gao Lei(高 磊)[b)], Li Chao-Rong(李超荣)[c)], and Ji Ai-Ling(纪爱玲)[b)†]

[a)] *Information Engineering School, Hangzhou Dianzi University, Hangzhou* 310018, *China*
[b)] *State Key Laboratory for Surface Physics, Institute of Physics, Chinese Academy of Sciences, Beijing* 100190, *China*
[c)] *School of Sciences, Zhejiang Sci-Tech University, Hangzhou* 310018, *China*

(Received 26 January 2013; revised manuscript received 19 April 2013)

Thin films of ternary compounds Cu_xIn_yN and Cu_xTi_yN were grown by magnetron sputtering to improve the thermal stability of Cu_3N, a material that decomposes below 300 °C, and thus promises many interesting applications in direct-writing. The effect of In or Ti incorporation in altering the structure and physical properties of copper nitride was evaluated by characterizing the film structure, surface morphology, and temperature dependence of electrical resistivity. More Ti than In can be accommodated by copper nitride without completely deteriorating the Cu_3N lattice. A small amount of In or Ti can improve the crystallinity, and consequently the surface morphology. While the decomposition temperature is rarely influenced by In, the Ti-doped sample, $Cu_{59.31}Ti_{2.64}N_{38.05}$, shows an X-ray diffraction pattern dominated by characteristic Cu_3N peaks, even after annealing at 500 °C. Both In and Ti reduce the bandgap of the original Cu_3N phase, resulting in a smaller electrical resistivity at room temperature. The samples with more Ti content manifest metal–semiconductor transition when cooled from room temperature down to 50 K. These results can be useful in improving the applicability of copper–nitride-based thin films.

Keywords: ternary nitride, thin film, thermal stability, electrical properties

PACS: 68.55.Jk, 73.50.Bk, 81.05.Hd **DOI:** 10.1088/1674-1056/22/6/066804

1. Introduction

Over the past decade there has been intensive interest in the synthesis of copper–nitride films due to their low decomposition temperature, a characteristic which promises many intriguing applications in fields such as high density optical storage,[1,2] microelectronics,[3,4] and solar energy technology.[5] The metastability of copper nitride can be used, for example, for patterning and metallization of other functional layers by various methods, in particular by direct-writing with electron or laser beam.[1,2,6,7] On the other hand, however, the low decomposition temperature is detrimental to the sample preparation, characterization, and device design. Consequently it is highly desirable to raise the decomposition temperature of copper nitride while maintaining the useful characteristics favorable for the above-mentioned applications.

Reported decomposition temperatures of copper nitride in the early publications show a large discrepancy, i.e., scattered in a wide range from 100 °C–300 °C.[2,3,6,8–11] This is quite understandable since often the tested samples were non-stoichiometric, and the samples are also vulnerable to the energetic particles applied in some characterizing procedures. By carefully optimizing the growth conditions, the current authors have obtained stoichiometric Cu_3N samples from which the first transmission electron microscopic (TEM) image was obtained,[12] and the decomposition temperature was determined to be slightly over 300 °C,[11] judging by the appearance of the Cu-peak on the X-ray diffraction (XRD) pattern for the annealed samples.

The decomposition temperature of Cu_3N is anticipated to be raised by doping with some other metal elements that have a stronger bonding to N atoms.[13,14] In this effort we wish the lattice structure of the matrix Cu_3N would not be seriously distorted, and the decomposition product, now an alloy of a doping metal with Cu, still features an electrical conductivity comparable with Cu. Cu_3N has a rather open anti-ReO_3 structure,[15] a rare property that can be also found in Na_3N.[16,17] The large cuboctahedral void is believed to be able to accommodate an excess atom of Cu or another element to yield an anti-perovskite type structure. In actual fact this is often not the case. Depending on the nature of the additional atom, the Cu_3N lattice will be destroyed, and consequently no solid or thin film samples can be obtained when a critical fraction of its unit cells is occupied by an additional atom. The incorporation of a foreign metal can significantly modify the energy band structure, bringing a remarkably change in the thermal stability, the optical and electrical properties of this material. Various metals, such as lithium, palladium, and sil-

*Project supported by the National Natural Science Foundation of China (Grant Nos. 51172272, 10904165, and 11290161) and the National Basic Research Program of China (Grant No. 2012CB933002).

†Corresponding author. E-mail: alji@iphy.ac.cn

© 2013 Chinese Physical Society and IOP Publishing Ltd

ver, have been applied to obtain Cu_3NM_x thin films,[18–25] in which some interesting new properties have been measured. Remarkably, in the $Cu_3NPd_{0.238}$ sample a constant electrical resisitivity over a temperature range of more than 200 °C has been achieved.[26] Frustrating as it may be, the decomposition temperature of such Cu_3NM_x thin films sees no satisfactory improvement in comparison to the stoichiometric Cu_3N. Light doping with O atoms raises the decomposition temperature of Cu_3N films to 360 °C,[11] but the electrical conductivity of the decomposition product drops sharply. Moreover, to dope copper nitride is a hard job. More effort should be devoted to the search for metals that can raise the decomposition temperature of copper nitride, while on the side, providing some new and interesting properties in the ternary compounds.

This work is based on our previous practice on the growth and investigation of stoichiometric Cu_3N and ternary Cu_3NM_x films,[11,12,26–29] wherein the foreign metal atoms are expected to occupy the center of the cubic lattice of the anti-ReO_3 structure. Two elements, In and Ti, were chosen to grow Cu_3N-based ternary compounds. In so doing, the content of the foreign elements is increased to an extent that the Cu_3N lattice is completely distorted, and thus either no stable compound is available or the deposit transitions to other phase. The influence of the foreign elements on the thermal stability, crystallinity, and surface morphology, and more importantly, the electrical resistivity of the deposits has been thoroughly investigated. It can be seen that with a reasonably small amount of Ti the crystallinity and thermal stability of the deposits can be significantly improved.

2. Experimental

Ternary Cu_xIn_yN and Cu_xTi_yN thin films were grown on Si (100) substrate by using an RF (27.12 MHz) magnetron sputtering method. The working gas is high-purity (5N) nitrogen, and the target consists of M-metal (M = In, Ti) slices welded on a Cu disk (ϕ60 mm) in a symmetrical configuration. In order to obtain films with different M-metal contents, the area of the M-metal is variable. The power supply was set at 60 W so as to favor the formation of weak Cu–N bonds. The substrates were ultrasonically cleaned successively in alcohol, acetone, and deionized water before mounting in a vacuum, and the distance between substrate holder and the target was fixed at 55 mm. After the chamber was evacuated to a base pressure of less than 6×10^{-6} mbar (1 bar = 10^5 Pa), nitrogen gas was introduced into the growth chamber to maintain a working pressure of 6.7×10^{-3} mbar. No intentional heating of the substrate was applied. For all the deposits here concerned, the growth time is 30 min.

The nominal composition of the deposits was characterized by energy-dispersive X-ray spectrometry performed on a scanning electron microscope (SEM, XL30) which also served for the morphology evaluation of the deposits. The accuracy for the compositions thus obtained is roughly 1.0%. The crystal structure of the deposits was determined by XRD (M18AHF) using the Cu Kα radiation ($\lambda = 1.5406$ Å). Thermal stability of the deposits was evaluated via XRD measurement carried out on samples annealed under N_2 protection for 20 min at various temperatures. The electrical resistivity of the deposits was measured using the conventional four-point probe method.

3. Results and discussion

The XRD patterns of the ternary Cu_xIn_yN and Cu_xTi_yN films in various compositions are presented in Figs. 1 and 2. In the case of Cu_xIn_yN, one can see that with the content of In increasing to 8.2%, i.e., in the sample $Cu_{52.65}In_{8.20}N_{39.15}$, the (001) and (002) reflections characterizing the Cu_3N lattice are still recognizable, see curves (*a*–*c*) in Fig. 1. On curve *d* for the sample $Cu_{49.28}In_{10.79}N_{39.93}$, the Cu_3N (001) and (002) reflections disappeared, but that for the Cu_3N (111) reflection of a negligibly small intensity is visible. With more In incorporated into the deposit, the InN (002) reflection becomes visible, see curve *e*. Thus we can say with confidence that in the case of Cu_xIn_yN, the Cu_3N lattice can be still preserved when the content of In is below ∼ 9.0 at%. A similar situation occurs in Cu_xIn_yN. The (001) and (002) reflections of Cu_3N are well preserved when the content of Ti is up to 11.1 at% (curves *a*–*d* in Fig. 2). It is in the sample $Cu_{37.28}Ti_{20.60}N_{42.12}$ that the (001) and (002) reflections of Cu_3N almost completely disappear. In the cases of heavier doping shown in Figs. 2(c)–2(e), the films comprise very tiny crystallites of variable compositions or structures, so microanalysis of the lattice structure and composition by transmission electron microscope is necessary to determine the features of the deposits accurately.

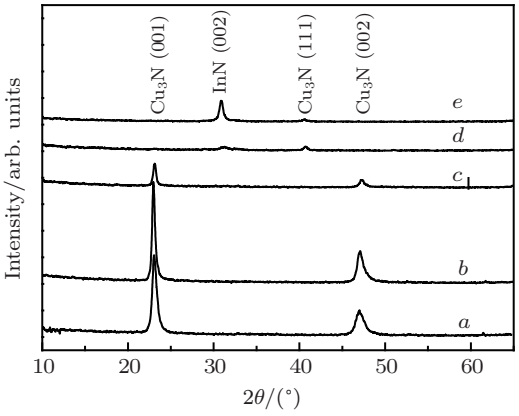


Fig. 1. XRD patterns for the films of copper–indium–nitride with various amounts of indium: (a) $Cu_{67.42}N_{32.58}$, (b) $Cu_{60.47}In_{4.62}N_{34.91}$, (c) $Cu_{52.65}In_{8.2}N_{39.15}$, (d) $Cu_{49.28}$ $In_{10.79}N_{39.93}$, and (e) $Cu_{42.37}In_{23.64}N_{33.99}$.

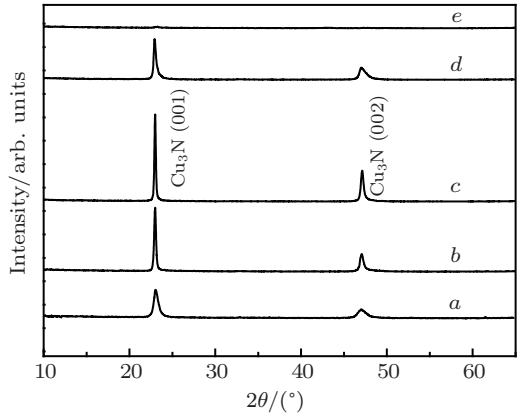


Fig. 2. XRD patterns for the films of copper–titanium–nitride of various amounts of titantium: (a) $Cu_{67.56}N_{32.44}$, (b) $Cu_{59.31}Ti_{2.64}N_{38.05}$, (c) $Cu_{51.66}Ti_{5.84}N_{42.50}$, (d) $Cu_{41.43}Ti_{11.10}N_{47.47}$, and (e) $Cu_{37.28}Ti_{20.60}N_{42.12}$.

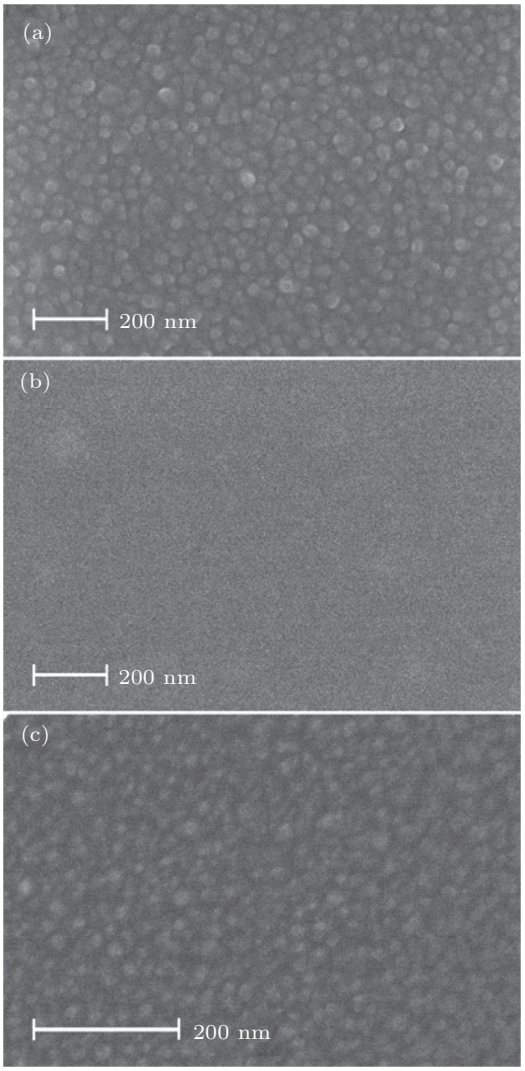


Fig. 3. Surface morphology under SEM of copper–indium–nitride with varied In contents, of which the characteristic diffraction pattern of Cu_3N lattice is still preserved: (a) $Cu_{67.42}N_{32.58}$, (b) $Cu_{60.47}In_{4.62}N_{34.91}$, and (c) $Cu_{49.28}In_{10.79}N_{39.93}$.

Some other interesting features concerning those Ti- and In-doped Cu_3N samples, in the sense that the (001) and (002) reflections of Cu_3N lattice are still preserved, are noteworthy.

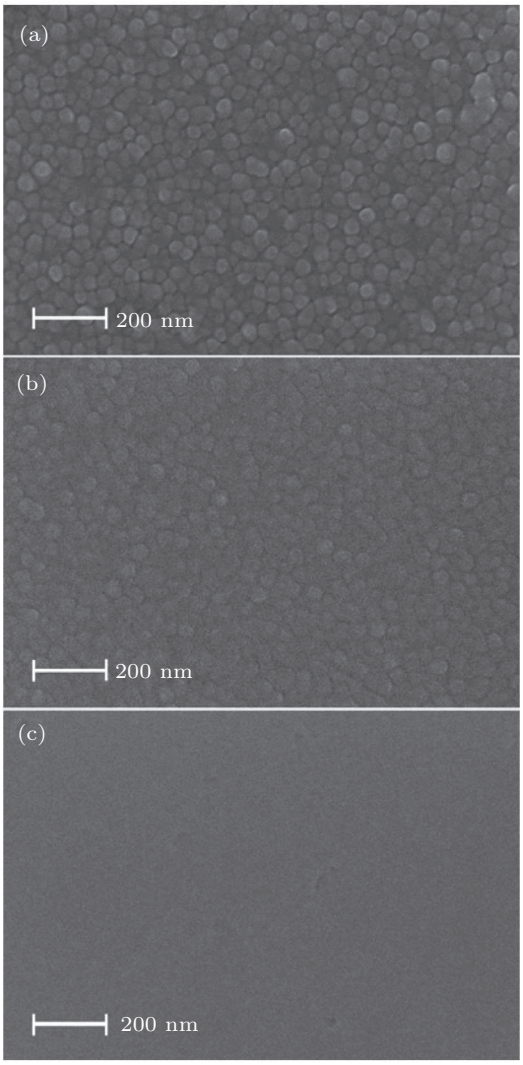


Fig. 4. Surface morphology under SEM of copper–titanium–nitride with varied Ti contents: (a) $Cu_{67.56}N_{32.44}$, (b) $Cu_{51.66}Ti_{5.84}N_{42.50}$, and (c) $Cu_{41.43}Ti_{11.10}N_{47.47}$.

When only a slight amount of Ti or In is incorporated, comparing curve *b* with curve *a* in Fig. 1 and curve *c* with curve *a* in Fig. 2, the crystallinity of the deposit becomes well improved, in that, besides the obviously enhanced intensity, the half-width for the (001) reflection changes from $\Delta\theta \sim 0.57^\circ \sim 0.60^\circ$ for pure Cu_3N (at $2\theta = 23.05^\circ$) to $\Delta\theta \sim 0.40^\circ$, at $2\theta = 22.96^\circ$ for $Cu_{60.47}In_{4.62}N_{34.91}$, and to $\Delta\theta \sim 0.20^\circ$ at $2\theta = 22.99^\circ$ for $Cu_{51.66}Ti_{5.84}N_{42.50}$, respectively. This point is also confirmed by the morphology of the deposits, as the films with a small amount of Ti or In incorporated become smoother and more compact (i.e. Figs. 3(b), 3(c), 4(b), and 4(c)) in contrast to the nearly stoichiometric pure Cu_3N samples which show distinct pyramid-like crystallites of sizes between 30 nm and 50 nm (Figs. 3(a) and 4(a)). That the surface assumes a smoother morphology in Fig. 3(b), while in the corresponding sample the crystallites are larger, may be attributed to the fact that the Cu_3N crystallites are generally coated by an amorphous layer of pure metal atoms. For the discussion of the structure and morphology of crystallites for pure Cu_3N, read-

ers can consult our previous publications.[12,27,28] Similar texture change has also been encountered in copper–nitride films when the content of the additional oxygen comes to a critical value of $\sim 11\%$.[11] The above results indicate that a small amount of Ti or In can improve the quality of copper–nitride deposits, and in this aspect Ti is preferable. The stronger Ti–N bond may be the reason underlying this observation.

It is also noticeable that with increasing Ti (In) content, the content of Cu decreases, while that of nitrogen first experiences an increase (to ~ 47.47 at% in $Cu_{41.43}Ti_{11.10}N_{47.47}$) and then drops down. This implies that the presence of the foreign Ti (In) atoms, when the content is small, helps bond more nitrogen. This is helpful to overcome the cracking tendency of the original Cu_3N, which is often N deficient, depending on the preparation method. Further addition of Ti (In) will gradually deteriorate the Cu_3N structure. Accordingly, the deposit first sees an improved crystallinity and then becomes deteriorated.

Thermal stability of the copper–titanium (indium) nitride deposits was evaluated by annealing under the protection of N_2 gas each for 20 min at different temperatures. The annealing temperature under which the characteristic (111) peak for metallic Cu appears on the XRD pattern is taken as the decomposition temperature of the sample. Figure 5 displays the XRD patterns for three $Cu_{52.65}$ $In_{8.2}N_{39.15}$ samples, the as-deposited and two annealed under 330 °C and 360 °C. Obviously, for the sample annealed under 360 °C, the (001) and (002) reflections of Cu_3N become weakened and broadened while the (111) reflection of Cu begins to be visible. Compared with the result on the stoichiometric Cu_3N,[11] no considerable improvement to the thermal stability of Cu_3N has been achieved.

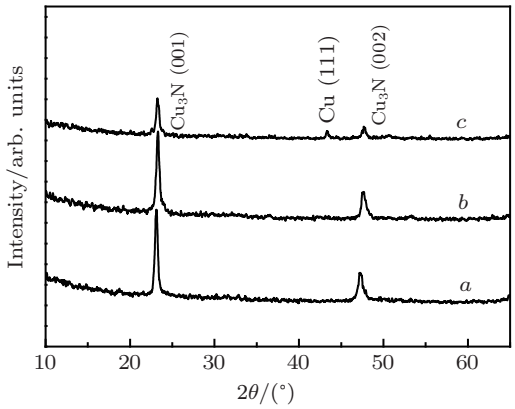


Fig. 5. XRD patterns for the film $Cu_{52.65}In_{8.2}N_{39.15}$: (a) as deposited, and annealed at (b) 330 °C, and (c) 360 °C.

In contrast, Ti seems more effective in raising the decomposition temperature of copper–nitride. In Fig. 6, the XRD patterns for the samples of $Cu_{59.31}Ti_{2.64}N_{38.05}$ are shown, as deposited and annealed at 350 °C to 500 °C. It can be seen that although the Cu (111) peak begins to be visible already at 400 °C, on curve *e*, corresponding to the sample annealed at 500 °C, the (001) and (002) peaks of Cu_3N are still the dominant features. With a little more Ti incorporated, the results are quite similar. This is to say that the incorporation of just a small amount of Ti can significantly raise the decomposition temperature of copper–nitride and make the decomposition proceed quite slowly. This explains why a much higher decomposition temperature was measured for Cu_3NTi_x by the thermal gravity and thermal enthalpy methods.

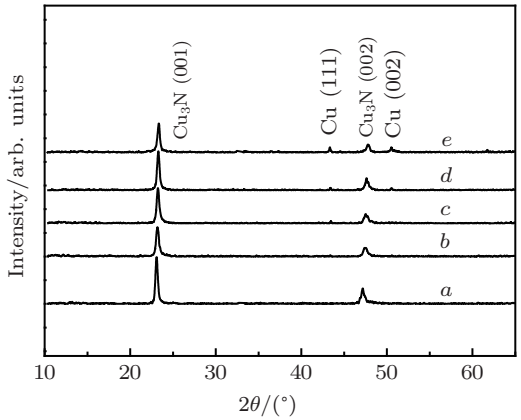


Fig. 6. XRD patterns for the samples of $Cu_{59.31}Ti_{2.64}N_{38.05}$: (a) as deposited, and annealed at (b) 350 °C, (c) 400 °C, (d) 450 °C, and (e) 500 °C.

The incorporation of a small amount of excess metal also significantly alters the electrical properties of copper–nitride. We measured the temperature dependence of the electrical resistivity for some Cu_xIn_yN and Cu_xTi_yN films, as represented in Figs. 7 and 8. As is well known, Cu_3N is a typical semiconductor, thus the temperature dependence of electrical resistively is a typical exponential curve.[12] The incorporation of a small amount of excessive metal atoms, also that of Cu itself, generally reduces the band gap, thus bringing down the activation energy for carriers to result in a lower electrical resistivity. In Fig. 7, the temperature dependence of electrical resistivity for the sample $Cu_{60.47}In_{4.62}N_{34.91}$ is presented, from which the activation energy E_a is calculated, based on the equation $\rho = \rho_0 \exp(E_a/kT)$, to be 6.86 meV, which is smaller than the 21.9 meV calculated for the stoichiometric Cu_3N sample.

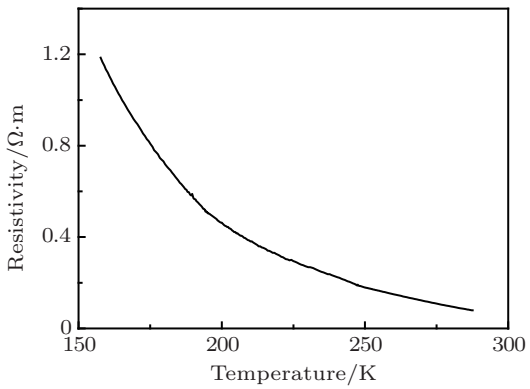


Fig. 7. Temperature dependence of electrical resistance for the as-deposited $Cu_{60.47}In_{4.62}N_{34.91}$ sample.

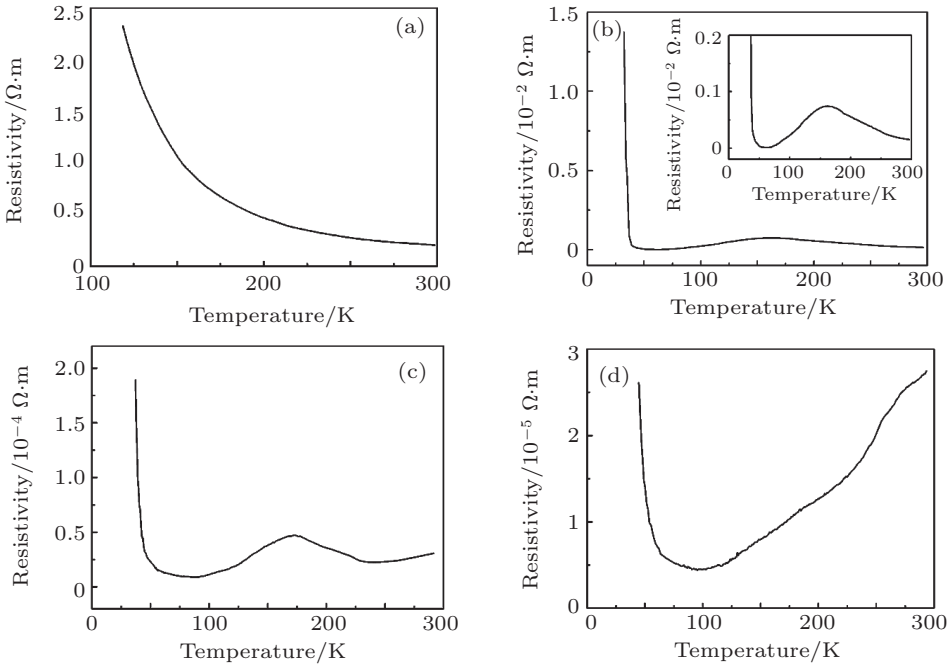


Fig. 8. Temperature dependence of electrical resistance for as-deposited copper–titanium–nitride with varied Ti contents: (a) $Cu_{61.76}Ti_{0.73}N_{37.51}$, (b) $Cu_{59.31}Ti_{2.64}N_{38.05}$, (c) $Cu_{51.66}Ti_{5.84}N_{42.50}$, and (d) $Cu_{41.43}Ti_{11.10}N_{47.47}$.

As more Ti can be incorporated into the Cu_3N lattice, consequently the situation is somewhat more complicated. The temperature dependence of electrical resistivity for four copper–titanium–nitride samples, namely $Cu_{61.76}Ti_{0.73}N_{37.51}$, $Cu_{59.31}Ti_{2.64}N_{38.05}$, $Cu_{51.66}Ti_{5.84}N_{42.50}$, and $Cu_{41.43}Ti_{11.10}N_{47.47}$, were measured (Fig. 8). With a Ti content of only 5.8 at%, the room temperature electrical resistivity has been rapidly brought down to 3×10^{-5} Ω·m from 3×10^{-2} Ω·m for stoichiometric Cu_3N. While the curve for the sample $Cu_{61.76}Ti_{0.73}N_{37.51}$, as that for $Cu_{60.47}$ $In_{4.62}N_{34.91}$ in Fig. 7, remains a monotonously exponential one, which characterizes the stoichiometric Cu_3N (Fig. 8(a)), a hunchback structure is visible on the curves in Figs. 8(b) and 8(c) indicating the occurrence of metal–semiconductor transition following the variation of temperature. These samples finally behave like an intrinsic semiconductor at $\sim$ 50 K with the electrical resistance growing steeply to surmount the detection limit within 10 K or so. Understanding the true mechanism underlying the variation of the electrical resistance with temperature, which is related to the metal–semiconductor transition here, requires knowledge of band structure of samples under consideration, which is, however, very difficult to calculate for these nonstoichiometric solids.

4. Conclusions

In summary, polycrystalline films of ternary compounds Cu_xIn_yN and Cu_xTi_yN of various compositions have been prepared by a magnetron co-sputtering method. By characterizing the film structure, of both as-deposited and annealed samples, and surface morphology, and measuring the temperature dependence of electrical resistivity, the effect of In and Ti incorporation in altering the structure and physical properties of copper–nitride have been evaluated. More Ti than In can be accommodated by copper–nitride without completely deteriorating the Cu_3N lattice. A small amount of In or Ti can improve the crystallinity and thus the surface morphology of the copper–nitride samples. While In has no essential effect in raising the decomposition temperature of copper–nitride, the Ti-doped sample $Cu_{59.31}Ti_{2.64}N_{38.05}$, even annealed at 500 °C, shows an XRD pattern dominated by the characteristic peaks of the Cu_3N lattice. Both In and Ti can reduce the bandgap of the original Cu_3N phase, thus bringing down the activation energy for carriers and the room temperature electrical resistivity. The samples with more Ti content manifest a metal–semiconductor transition within the temperature range from 50 K to room temperature. These results can be useful in employing copper–nitride-based thin films in many innovative applications.

References

[1] Asano M, Umeda K and Tasaki A 1990 *Jpn. J. Appl. Phys.* **29** 1985
[2] Maruyama T and Morishita T 1996 *Appl. Phys. Lett.* **69** 890
[3] Borsa D M, Grachev S, Presura C and Boerma D O 2002 *Appl. Phys. Lett.* **80** 1823
[4] Nosaka T, Yoshitake M, Okamoto A, Ogawa S and Nakayama Y 2001 *Appl. Surf. Sci.* **169** 358
[5] Navio C, Capitan M J, Alvarez J, Yndurain F and Miranda R 2007 *Phys. Rev. B* **76** 085105
[6] Maya L 1993 *J. Vac. Sci. Technol. A* **11** 604
[7] Cremer R, Witthaut M, Neuschutz D, Trappe C, Laurenzis M, Winkle O and Kurz H 2000 *Mikro. Acta* **133** 299
[8] Maruyama T and Morishita T 1996 *Appl. Phys. Lett.* **69** 890

[9] Nosaka T, Yoshitake M, Okamoto A, Ogawa S and Nakayama Y 2001 *Appl. Surf. Sci.* **169** 358
[10] Liu Z Q, Wang W J, Wang T M, Chao S and Zheng S K 1998 *Thin Solid Films* **325** 55
[11] Du Y, Huang R, Ma L B, Ji A L, Song R and Cao Z X, 2007 *J. Mater. Res.* **22** 3052
[12] Ji A L, Huang R, Du Y, Li C R and Cao Z X 2006 *J. Crystal Growth* **295** 79
[13] Zhou Z F, Qin F W, Zang H R, Zhang D, Chen W J, Zhi A B, Liu X L, Yu B and Jiang X 2011 *Chin. Phys. Lett.* **28** 028102
[14] Niu E W, Fan S H, Li L, Lu G H, Feng W R, Zhang G L and Yang S Z 2006 *Chin. Phys. Lett.* **23** 1533
[15] Juza R, Hahn H and Anorg Z 1938 *Allg. Chem.* **239** 282
[16] Fischer D and Jansen M 2002 *Angew. Chem. Int. Ed.* **41** 1755
[17] Vajenine G V 2007 *Inorg. Chem.* **46** 5146
[18] Moreno-Armenta M G, Lopez W and Takeuchi N 2007 *Solid State Sci.* **9** 166
[19] Zachwiecha U and Jacobs H 1991 *J. Less-Common Met.* **170** 185
[20] Blucher J and Bang K 1989 *Mater. Sci. Eng. A* **117** L1
[21] Hayashi Y, Ishikawa T and Shimokawa D 2002 *J. Alloys Compd.* **330–332** 348
[22] Pierson J F and Horwat D 2008 *Scr. Mater.* **58** 568
[23] Gao L, Ji A L, Zhang W B and Cao Z X 2011 *J. Crystal Growth* **321** 157
[24] Ji A L, Du Y, Gao L and Cao Z X 2010 *Phys. Status Solidi A* **207** 2769
[25] Gulo F, Simon A, Kohler J and Kremer R K 2004 *Agew. Chem. Int. Ed.* **43** 2032
[26] Ji A L, Li C R and Cao Z X 2006 *Appl. Phys. Lett.* **89** 252120
[27] Ji A L, Li C R, Du Y, Ma L B, Song R and Cao Z X 2005 *Nanotech.* **16** 2092
[28] Du Y, Ji A L, Ma L B, Wang Y Q and Cao Z X 2005 *J. Crystal Growth* **280** 480
[29] Ji A L, Du Y, Li C R and Cao Z X 2007 *J. Vac. Sci. Technol. B* **25** 208